What is the best anchoring group for a dye in a dye-sensitized solar cell?

ARTICLE *in* JOURNAL OF PHYSICAL CHEMISTRY LETTERS · MAY 2012

Impact Factor: 7.46

1 AUTHOR:

Natalia Martsinovich
The University of Sheffield
60 PUBLICATIONS **868** CITATIONS

SEE PROFILE

THE JOURNAL OF PHYSICAL CHEMISTRY Letters

Letter

pubs.acs.org/JPCL

What Is the Best Anchoring Group for a Dye in a Dye-Sensitized Solar Cell?

Francesco Ambrosio, Natalia Martsinovich, and Alessandro Troisi*

Department of Chemistry and Centre of Scientific Computing, University of Warwick, CV4 7AL Coventry, U.K.

Supporting Information

ABSTRACT: We developed a computational procedure to screen many different anchoring groups used or usable to connect a dye to the semiconducting surface in a dye-sensitized solar cell. The procedure leads to a clear identification of the anchoring groups that bind strongly to the surface and facilitate the electron injection at the same time, providing clear-cut indications for the design of new dyes. The complicated interplay of factors that determine the final results (preferred adsorption mode, the anchor's effect on the dye's electronic structure, and dye−semiconductor coupling) is illustrated through a few examples showing how chemical intuition can often be misleading in this problem.

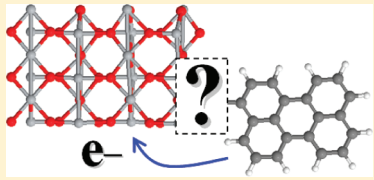

SECTION: Energy Conversion and Storage; Energy and Charge Transport

Improving the efficiency of dye-sensitized solar cells (DSSC),[1−3] one of the new most promising phothovoltaic technologies, is very challenging because each one of their components (nanocrystalline TiO_2, dye adsorbed on TiO_2, electrolyte or solid state hole transporter, additives, and electrodes) cannot be improved independently from all of the others. For example, a good dye should (i) be stably bound to the semiconductor surface, (ii) absorb solar radiation, (ii) in its photoexcited state inject very rapidly the electron into TiO_2, (iii) be easily regenerated by the redox pair in solution (or the hole transporting material), (iv) avoid photodegradation, and (v) recombine as slowly as possible with the electrons in the semiconductor when oxidized. This very long list of requirements is even more complicated to satisfy if we consider that by simply changing the additive[4,5] or the redox couple[6] in the cell, the energetics of the interface and therefore the electron-transfer kinetics is completely changed, and the best dye in some experiment is not necessarily the best in some other. The current research efforts include so many different directions (synthesis of new dyes, exploration of new electrolytes, hole conducting materials, and additives) that, clearly, there are no established "optimal" components of the DSSC yet.

Since the first investigations of DSSC, computational chemistry has been used to disentangle some of the phenomena that are relevant to the functioning of DSSC and to introduce an element of design in the systematic exploration.[7] Excellent results have been achieved in the calculation of the absorption spectra[8] and the geometry of the dyes adsorbed on the semiconductor.[9,10] A range of methodologies have been proposed to compute the electron injection rate,[11−13] providing results of different accuracy, all limited to some extent by the inability of predicting the alignment of the energy levels of the dye and the semiconductor in the presence of a complex liquid−solid interface (in addition to the DFT limitations, which can, in principle, be reduced). The difficulty in computing this energy level alignment is also one of the main inaccuracies when one attempts to compute the charge recombination rate.[14] We show in this paper that, notwithstanding the current limitations of computational chemistry methods, it is possible to define with a good degree of confidence at least one of the chemical characteristics of the solar cell, the anchoring group that connects the dye to the semiconductor.

The anchoring group determines the binding energy of the dye on TiO_2 (largely affecting its long-term stability) and the injection rate (through mediating the electron transfer from the chromophore to the semiconductor) and can also modulate the injection energy by altering the energy of the dye's excited state. Introducing alternative anchoring groups can be synthetically laborious, and in the absence of alternative indications, the vast majority of dyes are anchored to TiO_2 with the carboxylic[1] and, sometimes, phosphonic[15] acid groups.

It is relatively straightforward to compute the binding energy of different anchoring groups.[16,17] On the other hand, the injection rate is affected by the dye's anchoring group in two ways, through the electronic coupling between the dye and the semiconductor, mediated by the anchor group, and through the position of the dye's virtual orbital and its energy alignment with the TiO_2 conduction band. The former is the inherent property of the anchoring group, while the latter (the energy of the dye's virtual orbital) can also be altered by varying other functional groups in the dye, and its evaluation is also affected by the uncertainty in the computation of energy levels. Therefore, calculating the injection energy for a dye connected to TiO_2 through different anchoring groups will *not* provide a good indication of the inherent propensity of the anchoring group to facilitate the charge injection because it will include the effect both of the semiconductor−dye coupling and of the

Received: April 27, 2012
Accepted: May 18, 2012

   dx.doi.org/10.1021/jz300520p | *J. Phys. Chem. Lett.* 2012, 3, 1531−1535

variable injection energy. However, by a simple adaptation of our recently introduced method[7] for the computation of the charge injection time, it is possible to compute the injection time for dyes connected through different anchoring groups assuming (imposing) a constant energy level alignment between the dye and semiconductor levels. In other words, it is possible to compare computationally the effect of changing *only* the anchoring group, obtaining insight that a collection of experiments or straightforward computations cannot achieve. As discussed more extensively in ref 7, fast injection is a necessary but not sufficient condition for high power conversion efficiencies (PCEs). We stress that this Letter will identify anchoring groups with fast injection rather than high PCE, the latter being determined by the combination of all processes in the cell.

In this work, we consider a series of dyes that have the same aromatic part (perylene) but various anchoring groups, illustrated in Figure 1 and labeled from (a) to (o), which will

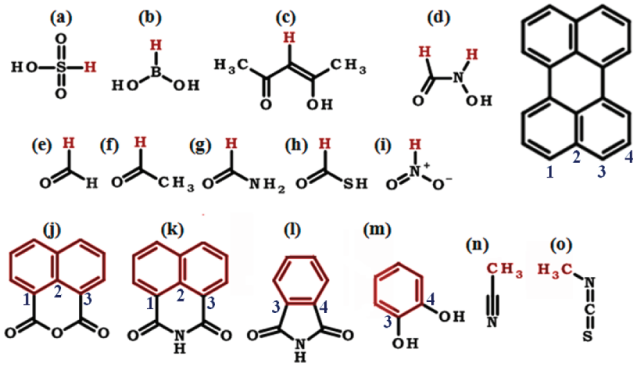

Figure 1. (a–o) Molecules with model anchoring groups studied in this work for the calculation of the binding energy. For the calculation of the injection time, these molecules have been modified to include the perylene dye. In (a)–(j), the H atom in red was substituted with the perylene connected via the carbon in position 1 (for molecules in (d), two separate dyes have been considered by substituting selectively only one of the two H atoms). For (j)–(m), the aromatic portion in red was augmented to give the full perylene structure, keeping the indicated atom numbering of the perylene. For (n) and (o), the methyl group was substituted with the perylene, connected with the anchoring group from position 1.

be considered together with the previous results on carboxylic and phosphonic acid binding groups.[7,18] Perylene was chosen as it is a common reference for spectroscopic and computational studies and it is often used for fundamental studies of electron transfer in DSSC-related systems.[11,15] Perylene itself is not a very efficient DSSC dye compared to dyes with a donor–π-acceptor structure, which offer better PCE.[3] However, our study aims to be almost independent of the choice of the dye and should be relevant to any organic dye containing one anchoring group.

The choice of anchoring groups is based on the available literature and several chemical considerations, as described below. Sulfonic acid anchors (a) have been used in ref 19 with hemicyanine and merocyanine dyes; a modified N3 dye with a boronic acid linker (b) has been reported;[20] acetylacetone (c) and hydroxamic acid (d) groups have been used for TiO_2 nanoparticle functionalization and to connect Mn(II) complexes to the TiO_2 surface;[21,22] (e–i) are studied here to make a detailed comparison between carboxylic acid and the aldehyde, ketone, amine, thiocarboxylic acid and nitro group. The models (j) and (k) are studied to describe the adsorption on TiO_2 of anhydrides and imides present in the commonly used PTCDA and PTCDI dyes.[23−25] Structure (l) is first proposed as a DSSC dye in this work; its high acidity facilitates the adsorption of a proton on the semiconductor surface, thus favoring the formation of a Ti–N bond and a possible tridentate adsorption mode. Ruthenium complexes featuring (m) as the anchoring group were initially proposed in ref 26. Finally, we study (n) and (o) because the cyano (CN−) and isothiocyano (NCS−) moieties are often featured in both organic and metal–organic dyes[3] (including the solvent, acetonitrile, used in many DSSC), and by including them in the calculation, we can estimate their contribution to the dyes' surface binding energy and evaluate the possibility of electron injection mediated by them. We have not considered multiple anchoring groups as the number of possible adsorption modes may become very large and is, to a larger extent, dependent on the specific dye considered.

Computational Details. The method described in detail in ref 7 is employed to compute electron injection times. The charge injection is defined as a charge-transfer process between an orbital localized on the dye molecule ($|s\rangle$) and one of the one-electron states of the continuum formed by the semiconductor's conduction band states (the family of states $\{|l\rangle\}$). These orbitals can be expressed as a linear combination of atomic orbitals, $|s\rangle = \sum_m c_m\chi_m$ and $|l\rangle = \sum_k C_{kl}\phi_k$, localized on the dye and on the semiconductor, respectively. The rate of electron injection, Γ, can be expressed as

$$\hbar\Gamma = 2\pi \sum_{m,n} c_m c_n^* \sum_{k,k'} (ES_{mk} - V_{mk'})(ES_{nk} - V_{nk'})\rho_{kk'}(E_s)$$

Here, the matrix elements V_{mk} are defined as the electronic coupling between localized atomic orbitals on the semiconductor and on the dye, and S_{mk} are defined as the overlap matrix. The semiconductor's energy-dependent density matrix is defined as $\rho_{kk'}(E) = \sum_l C_{lk}C_{lk}\delta(E - E_l)$, where E_l are the energies of the one-electron states on the semiconductor. E_s is the injection energy (the LUMO energy of the dye is used). The quantities in the equation above can be obtained to a high degree of accuracy through a combination of separate calculations;[7] $\rho_{kk'}(E)$ is computed for the clean surface, $\{V_{mk}\}$ for a model system containing surface and anchoring groups, and $\{c_m\}$ is for an isolated dye's LUMO. This procedure of replacing the whole "surface + dye" system with a combination of smaller systems (surface, surface–anchoring group interface, and isolated dye) is particularly well suited to screening a large number of potential chromophores as it is much faster than calculations of an entire adsorbed dye. This approach stands in contrast to other recent theoretical studies of TiO_2–dye systems for DSSC,[9−13,27] which consider a complete dye adsorbed on the surface and are necessarily limited to studies of a few systems. For example, ref 27 reports differences in the adsorption geometry and electronic structure of two dyes containing carboxylic-acid-based anchoring groups. In this work, we exploit the partitioning scheme to consider the injection through a large number of anchoring groups without repeating the calculation of the full chromophore on the TiO_2 slab. As we want to consider the effect of the anchoring group on the TiO_2–dye coupling independently from its role in shifting the LUMO energy, we enforce the LUMO energy to be constant for each dye (0.4 eV above the conduction band edge). This also allows us to use a smaller slab than that in ref 7 (the thickness of the slab affects the position of the TiO_2

dx.doi.org/10.1021/jz300520p | J. Phys. Chem. Lett. 2012, 3, 1531–1535

conduction band and therefore the energy level alignment but not the dye−TiO_2 coupling).[28] This is not to be considered an approximation but a numerical strategy to separate the anchoring group's effect on the coupling and to factor out its effect on the LUMO energy. The Supporting Information (SI) reports the (similar) results obtained using the calculated dyes' LUMO energies. Another measure of how the anchor group can alter the dye's electronic structure is given by the variation in the computed absorption energy (also given in the SI). For the majority of dyes with different anchors, the lowest computed transition is in the narrow range between 2.61 and 2.79 eV. Outside of this range, we find the phthalimide and the nitro group (strongly red shifted at 2.44 and 2.51 eV) and one of the hydoxamic acids (d_C) at 2.88 eV.

All-electron quantum chemical calculations were performed with CRYSTAL09 code[29] using the B3LYP density functional and Gaussian basis set (triple valence plus polarization for Ti, O, and S and double valence plus polarization for C, N, B, and H). For the periodic calculations, the *k*-points sampled were chosen using a Monkhorst−Pack net with a 2 × 2 × 1 *k*-points grid. Rutile (110) and anatase (101) surfaces were modeled using slabs containing two Ti_2O_4 layers with the 2 × 2 or 2 × 4 cell area (the larger cell was used for the larger molecules (c), (i), (j) and (k)). The reported binding energies were corrected for the basis set superposition error. The methodology was validated in ref 7 by successfully comparing the computed injection times for perylenes and isonicotinic and bi-isonicotinic acid with femtosecond spectroscopy results; see, for example, refs 15 and 30.

We studied the attachment chemistry and computed the binding energies of 15 different anchoring groups on both anatase (101) and rutile (110) surfaces. Most of the groups have multiple stable adsorption modes, with different adsorption energies (see Table ST1 and Figures S1 and S2 (SI) for adsorption energies and geometries, respectively). For example, boronic acid on anatase (101) adsorbs in two monodentate configurations (i.e., with one oxygen in close contact with one Ti atom), one of which is dissociative (i.e., with one acidic hydrogen adsorbed on the surface as a separate atom) and one molecular (i.e., keeping the same chemical connectivity of the isolated molecule). The boronic acid also has four bridging bidentate adsorption modes (two oxygens of the molecule closely interact with two different Ti atoms), one of which is molecular and the other three dissociative. We have identified in total 35 adsorption modes on anatase (101) and 26 adsorption modes on rutile (110). For each anchoring group and each observed adsorption geometry, we computed the electron injection time, 1/Γ, for a perylene molecule bearing the group on anatase (101) and rutile (110). The full set of results is provided in the SI, while we focus here on the injection times for the most stable adsorption geometries.

In the top panel of Figure 2, we report a chart of the computed electron injection times of functionalized perylene molecules on anatase (101) versus the binding energy on the surface for each anchoring group in its most stable adsorption geometry. We have also reported (in lighter color) the data for the second most stable adsorption geometry if less than 4 kcal/mol higher in energy. To better evaluate the relative magnitudes of adsorption energies, the figure contains a horizontal dotted line corresponding to the binding energy of the carboxylic group (the most used anchoring group). The figure also reports for reference the binding energy for acetonitrile (the solvent used in DSSC) because binding

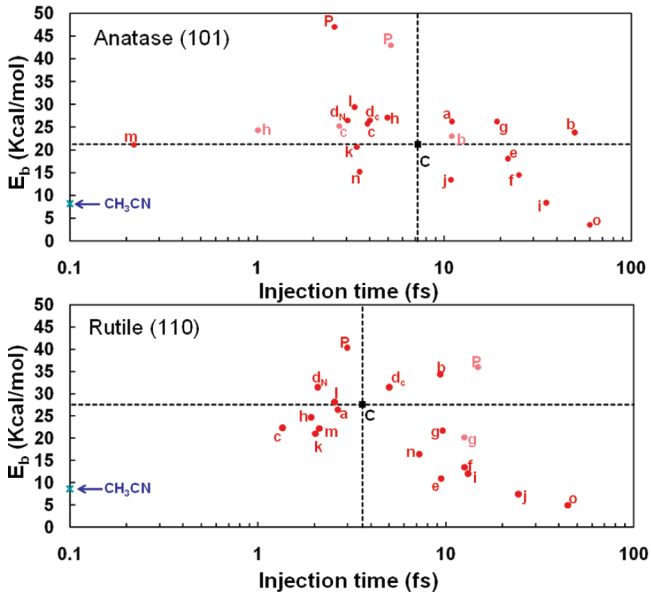

Figure 2. Electron injection times versus adsorption energy for different anchoring groups (a−o) for anatase (101) and rutile (110). Calculation of carboxylic acid (C) and phosponic acid (P) from refs 7 and 18 are included. The adsorption energy of the solvent (acetonitrile) is indicated for reference. The data points in red are for the most stable adsorption geometry, and those in lighter color are for the second most stable adsorption geometry (if within 4 kcal/mol).

energies close to or smaller than that of the solvent are clearly too low. In the same figure, we represent with a vertical dotted line the injection time of the perylene chromophore connected to TiO_2 though the carboxylic acid. This representation allows an immediate visualization, in the top left quadrant of the diagram, of the anchoring groups that can be considered promising alternatives to the common carboxylic acid. Anchoring groups outside of this quadrant should be discarded because they will be lacking in good properties of stability and/or injection. Some correlation between strong binding and fast injection can be observed in the figure, but this is too weak to be used for predicting one property from the other, and the results should be analyzed individually.

Acetylacetone (c) and hydroxamic acid (d) anchors display good computed binding and injection characteristics, in agreement with the experiments.[21,22] In particular, hydroxamic acid in its bridging bidentate configuration has a stable di-ionic form and features very fast injection when the dye is attached replacing the hydrogen bonded to the nitrogen atom. Catechol (m), in its bridging bidentate mode with two hydrogens donated to the surface, is the fastest injecting anchoring group (0.47 fs) due to the strong coupling given by the two oxydril groups directly linked to the aromatic core of the dye, with an adsorption energy similar to that of the carboxylic acid. The injection times of sulfonic (a) and boronic (b) acid are worse than that of the carboxylic acid (because of a low electron density of the LUMO on the atoms attached to the surface; see Figure 4), and the increase of adsorption energy is not enough to suggest their employment. This is to be contrasted with phosphonic acid (P) (studied in ref 18), which has good injection properties and the strongest adsorption energy. Anchoring groups (e)−(i) are included in this work as they all feature a simple modification of the common carboxylic acid. Somewhat expectedly, we find that the aldehyde (e) and the ketone (f) anchoring groups give a weaker binding and slower

dx.doi.org/10.1021/jz300520p | J. Phys. Chem. Lett. 2012, 3, 1531−1535

injection than the carboxylic acid; the lack of hydrogen bonds reduces the interaction with the surface and the coupling of the dye's LUMO with the conduction band of the semiconductor. The amide (g) has an increased binding energy (26.25 kcal/mol), but the effect of this anchoring group on electron injection is undesirable; due to its electron-donating characteristics, the LUMO is more localized on the aromatic core of the dye, leading to a slower injection.

The relative injection time, however, is affected not only by the LUMO shape. The comparison between the anchors (g) and (i) illustrates well the importance of the full computational scheme, including the coupling with the semiconducting substrate, in comparison with simple chemical intuition. The strongly electron withdrawing nitro group (i) would be expected to decrease the injection time, while the computed value is very large (35.20 fs) (considering its modest binding energy, this is a very poor anchoring group). On the opposite end within the (e)−(i) family, we find the thiocarboxylic acid (h) (4.98 fs). An inspection of the LUMO isodensity for the two dyes (Figure 4) does not explain the difference because

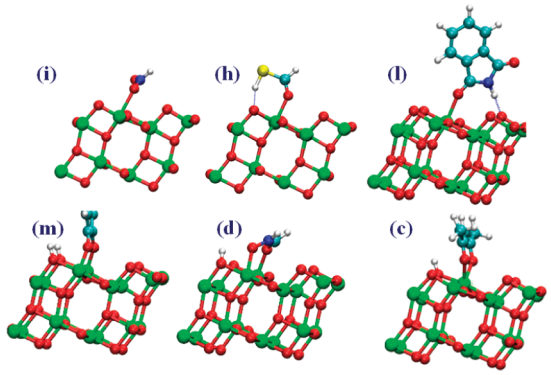

Figure 3. Illustration of several stable adsorption modes on anatase (101) for selected anchors. (i–l) are monodentate modes, (m,d) are bridging bidentate modes, and (c) is a chelating bidentate mode.

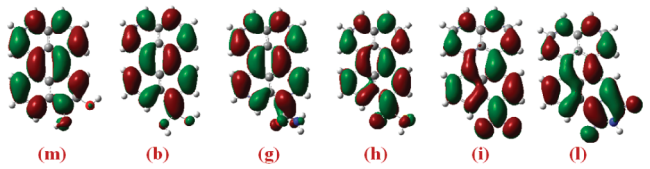

Figure 4. Isodensity representation of the LUMO orbital in the space for representative functionalized dyes (labeled as in Figure 1).

they are fairly similar, and the weight of the LUMO coefficients on the oxygen atom attaching to the TiO_2 surface (see Figure 3 for the anchor−slabs structures) is actually larger for the nitro group than that for the thio acid. Analyzing the terms entering in the rate equation, we observe in this case that the difference is due to a larger coupling of the thio acid with the TiO_2 orbitals (partially due to the S−Ti coupling and an additional hydrogen bond). This difference could not be predicted without an explicit calculation. Another clear example of the importance of calculations is the case of dye (m), which gives the fastest injection among all of the considered functionalized perylene molecules. We observe in this case the competition between two effects. The two oxydril groups featured in (m) are π-electron-donating groups, and the LUMO density on these two oxygen atoms is very low. However, when we look at the coupling between the dye and semiconductor atomic orbitals, we observe very strong coupling between Ti and C atoms in positions 3 and 4 (Figure 1), with moderate O−Ti coupling for oxygen connected to position 3. Overall, the (m) anchor modifies the LUMO density so that the injection time is reduced, but it also brings this density closer enough to the surface that the coupling effect dominates and the injection is overall much faster.

The characteristics of dianhydride and di-imide groups are studied through the model compounds (j–l). While the dianhydride moiety (j) is both weakly adsorbed and a slow injector, naphthalimide (k) and phtalimide (l) groups bind strongly to the semiconductor surface (20.67 and 29.43 kcal/mol, respectively) due to the imide's proton hydrogen bond with the surface oxygen, and they provide efficient electron injection for the related perylene molecules (~3.4 fs). The less strained geometry of the phtalimide bond with the surface is the likely reason for the different adsorption energy of the two different imides. Finally, our results show that the electron-withdrawing and electron-donating characteristics, respectively, of (n) (−CN) and (o) (−NCS) are reflected in the electron injection time for the corresponding dyes (3.3 and 55 fs). The large difference is also due to a strong N−Ti coupling of the −CN group, while the long S−Ti bond (2.90 Å) of the −NCS moiety prevents efficient coupling. We therefore conclude that, while both of these groups provide an increased stability to dyes featuring them in proximity of the surface, only the −CN group provides an efficient alternative pathway of injection. It should be remembered that these calculations provide the thermodynamic stability of the dye, not its long-term photostability in a working device. Of the functional groups considered here, however, only aldehydes and ketones are known to be photochemically unstable (due to the Norrish reaction), but they turn out to be uninteresting for DSSC applications.

The bottom panel of Figure 2 shows the analogous results obtained for the same anchoring groups on rutile (110) (the most stable surface of the rutile polymorph, less frequently occurring in DSSC). The trend observed is similar, but in this case, bridging bidentate adsorption modes are dominant, where allowed (see the SI for details), and this is reflected in increased electron injection efficiency for the anchoring groups that feature molecular monodentate modes on anatase (101) but bidentate modes on rutile (110). On rutile (110), the carboxylic acid has a much stronger binding energy (~27 kcal/mol) so that, while many anchoring groups feature faster electron injection, only hydroxamic acid (d_N) and phosphonic acid (P) are better anchoring groups here.

This work led to a constructive design rule in the form of a few promising anchoring groups for DSSC dyes (e.g., phosphonic acid, dihydroxyl, and some imides) that can be used in substitution of the carboxylic acid and that should be intrinsically better at facilitating one of the key DSSC processes, electron injection, regardless of the other dye and device parameters. Through a simple computational procedure, we were able to decouple the ability of an anchoring group to inject an electron from all other effects that can be observed when a dye is modified in an experiment or in a computation (e.g., alteration of the surface dipole, coverage, adsorption energy). The proposed methodology is particularly important as we have shown that some of the results are not easily predictable on the basis of chemical intuition alone because the electron injection rate is determined by the delicate balance between weights of the dye's LUMO and the orbital's couplings. While the former is due to the electron distribution

dx.doi.org/10.1021/jz300520p | J. Phys. Chem. Lett. 2012, 3, 1531−1535

of the dye, which can be intuitively predicted, the latter is influenced by the adsorption geometry and the surface electronic structure, which are much harder to guess.

■ ASSOCIATED CONTENT

Supporting Information

All of the computed adsorption modes (geometries and adsorption energies) and injection rates (at fixed injection energy and at an injection energy equal to the computed LUMO energy) for anatase (101) and rutile (110). The lowest three excitation energies and the respective oscillator strengths for the dyes with different anchor groups. This material is available free of charge via the Internet at http://pubs.acs.org.

■ AUTHOR INFORMATION

Notes

The authors declare no competing financial interest.

■ ACKNOWLEDGMENTS

We acknowledge the financial support of EPRSC and ERC.

■ REFERENCES

(1) Oregan, B.; Gratzel, M. A Low-Cost, High-Efficiency Solar Cell Based on Dye-Sensitized Colloidal TiO2 films. *Nature* **1991**, *353*, 737.
(2) Preat, J.; Jacquemin, D.; Perpete, E. A. Towards New Efficient Dye-Sensitised Solar Cells. *Energy Environ. Sci.* **2010**, *3*, 891.
(3) Martsinovich, N.; Troisi, A. Theoretical Studies of Dye-Sensitised Solar Cells: From Electronic Structure to Elementary Processes. *Energy Environ. Sci.* **2011**, *4*, 4473.
(4) Nazeeruddin, M. K.; Kay, A.; Rodicio, I.; Humphry-Baker, R.; Muller, E.; Liska, P.; Vlachopoulos, N.; Gratzel, M. Conversion of Light to Electricity by *cis*-X_2bis(2,2′-bipyridyl-4,4′-dicarboxylate)-ruthenium(II) Charge-Transfer Sensitizers (X = Cl^-, Br^-, I^-, CN^-, and SCN^-) on Nanocrystalline Titanium Dioxide Electrodes. *J. Am. Chem. Soc.* **1993**, *115*, 6382.
(5) Boschloo, G.; Haggman, L.; Hagfeldt, A. Quantification of the Effect of 4-Tert-butylpyridine Addition to I^-/I_3^- Redox Electrolytes in Dye-Sensitized Nanostructured TiO_2 Solar Cells. *J. Phys. Chem. B* **2006**, *110*, 13144.
(6) Yella, A.; Lee, H. W.; Tsao, H. N.; Yi, C. Y.; Chandiran, A. K. Porphyrin-Sensitized Solar Cells with Cobalt (II/III)-Based Redox Electrolyte Exceed 12% Efficiency (vol 334, pg 629, 2011). *Science* **2011**, *334*, 1203.
(7) Martsinovich, N.; Troisi, A. High-Throughput Computational Screening of Chromophores for Dye-Sensitized Solar Cells. *J. Phys. Chem. C* **2011**, *115*, 11781−11792.
(8) Jacquemin, D.; Wathelet, V.; Perpete, E. A.; Adamo, C. Extensive TD-DFT Benchmark: Singlet-Excited States of Organic Molecules. *J. Chem. Theory Comput.* **2009**, *5*, 2420.
(9) Schiffmann, F.; VandeVondele, J.; Hutter, J.; Wirz, R.; Urakawa, A.; Baiker, A. Protonation-Dependent Binding of Ruthenium Bipyridyl Complexes to the Anatase(101) Surface. *J. Phys. Chem. C* **2010**, *114*, 8398.
(10) De Angelis, F.; Fantacci, S.; Selloni, A.; Nazeeruddin, M. K.; Gratzel, M. First-Principles Modeling of the Adsorption Geometry and Electronic Structure of Ru(II) Dyes on Extended TiO_2 Substrates for Dye-Sensitized Solar Cell Applications. *J. Phys. Chem. C* **2010**, *114*, 6054.
(11) Li, J.; Nilsing, M.; Kondov, I.; Wang, H.; Persson, P.; Lunell, S.; Thoss, M. Dynamical Simulation of Photoinduced Electron Transfer Reactions in Dye-Semiconductor Systems with Different Anchor Groups. *J. Phys. Chem. C* **2008**, *112*, 12326−12333.
(12) Prezhdo, O. V.; Duncan, W. R.; Prezhdo, V. V. Dynamics of the Photoexcited Electron at the Chromophore−Semiconductor Interface. *Acc. Chem. Res.* **2008**, *41*, 339.
(13) Abuabara, S. G.; Rego, L. G. C.; Batista, V. S. Influence of Thermal Fluctuations on Interfacial Electron Transfer in Functionalized TiO_2 Semiconductors. *J. Am. Chem. Soc.* **2005**, *127*, 18234.
(14) Maggio, E.; Martsinovich, N.; Troisi, A. Evaluating Charge Recombination Rate in Dye-Sensitized Solar Cells from Electronic Structure Calculations. *J. Phys. Chem. C* **2012**, *116*, 7638.
(15) Gundlach, L.; Letzig, T.; Willig, F. Test of Theoretical Models for Ultrafast Heterogeneous Electron Transfer with Femtosecond Two-Photon Photoemission Data. *J. Chem. Sci.* **2009**, *121*, 561.
(16) Bates, S. P.; Kresse, G.; Gillan, M. J. The Adsorption and Dissociation of ROH Molecules on TiO_2(110). *Surf. Sci.* **1998**, *409*, 336.
(17) Luschtinetz, R.; Frenzel, J.; Milek, T.; Seifert, G. Adsorption of Phosphonic Acid at the TiO_2 Anatase (101) and Rutile (110) Surfaces. *J. Phys. Chem. C* **2009**, *113*, 5730.
(18) Ambrosio, F.; Martsinovich, N.; Troisi, A. Effect of the Anchoring Group on Electron Injection: Theoretical Study of Phosphonated Dyes for Dye-Sensitized Solar Cells. *J. Phys. Chem. C* **2012**, *116*, 2622.
(19) Wang, Z. S.; Li, F. Y.; Huang, C. H. Highly Efficient Sensitization of Nanocrystalline TiO_2 Films with Styryl Benzothiazolium Propylsulfonate. *Chem. Commun.* **2000**, 2063.
(20) Altobello, S.; Bignozzi, C. A.; Caramori, S.; Larramona, G.; Quici, S.; Marzanni, G.; Lakhmiri, R. Sensitization of TiO_2 with Ruthenium Complexes Containing Boronic Acid Functions. *J. Photochem. Photobiol., A* **2004**, *166*, 91.
(21) McNamara, W. R.; Snoeberger, R. C.; Li, G.; Schleicher, J. M.; Cady, C. W.; Poyatos, M.; Schmuttenmaer, C. A.; Crabtree, R. H.; Brudvig, G. W.; Batista, V. S. Acetylacetonate Anchors for Robust Functionalization of TiO_2 Nanoparticles with Mn(II)−Terpyridine Complexes. *J. Am. Chem. Soc.* **2008**, *130*, 14329.
(22) McNamara, W. R.; Snoeberger, R. C.; Li, G. H.; Richter, C.; Allen, L. J.; Milot, R. L.; Schmuttenmaer, C. A.; Crabtree, R. H.; Brudvig, G. W.; Batista, V. S. Hydroxamate Anchors for Water-Stable Attachment to TiO_2 Nanoparticles. *Energy Environ. Sci.* **2009**, *2*, 1173.
(23) Forrest, S. R. Organic−Inorganic Semiconductor Devices and 3,4,9,10-Perylenetetracarboxylic Dianhydride: An Early History of Organic Electronics. *J. Phys.: Condens. Matter* **2003**, *15*, S2599.
(24) Tautz, F. S. Structure and Bonding of Large Aromatic Molecules on Noble Metal Surfaces: The Example of PTCDA. *Prog. Surf. Sci.* **2007**, *82*, 479.
(25) Hardin, B. E.; Hoke, E. T.; Armstrong, P. B.; Yum, J. H.; Comte, P.; Torres, T.; Frechet, J. M. J.; Nazeeruddin, M. K.; Gratzel, M.; McGehee, M. D. Increased Light Harvesting in Dye-Sensitized Solar Cells with Energy Relay Dyes. *Nat. Photonics* **2009**, *3*, 406.
(26) Rice, C. R.; Ward, M. D.; Nazeeruddin, M. K.; Gratzel, M. Catechol as an Efficient Anchoring Group for Attachment of Ruthenium−Polypyridine Photosensitisers to Solar Cells Based on Nanocrystalline TiO_2 Films. *New J. Chem.* **2000**, *24*, 651.
(27) Pastore, M.; De Angelis, F. Computational Modelling of TiO_2 Surfaces Sensitized by Organic Dyes with Different Anchoring Groups: Adsorption Modes, Electronic Structure and Implication for Electron Injection/Recombination. *Phys. Chem. Chem. Phys.* **2012**, *14*, 920.
(28) Martsinovich, N.; Jones, D. R.; Troisi, A. Electroniic Structure of TiO_2 Surfaces and Effect of Molecular Adsorbates Using Different DFT Implementations. *J. Phys. Chem. C* **2010**, *114*, 22659.
(29) Dovesi, R.; Orlando, R.; Civalleri, B.; Roetti, C.; Saunders, V. R.; Zicovich-Wilson, C. M. CRYSTAL: A Computational Tool for the Ab Initio Study of the Electronic Properties of Crystals. *Z. Kristallogr.* **2005**, *220*, 571.
(30) Schnadt, J.; Bruhwiler, P. A.; Patthey, L.; O'Shea, J. N.; Sodergren, S.; Odelius, M.; Ahuja, R.; Karis, O.; Bassler, M.; Persson, P.; Siegbahn, H.; Lunell, S.; Martensson, N. Experimental Evidence for Sub-3-fs Charge Transfer from an Aromatic Adsorbate to a Semiconductor. *Nature* **2002**, *418*, 620.